Received: 12 February 2021 | Revised: 7 March 2021 | Accepted: 9 March 2021

DOI: 10.1002/aoc.6242

FULL PAPER

Applied Organometallic Chemistry WILEY

# Synthesis of (4R)-2-(3-hydroxyphenyl)thiazolidine-4-carboxylic acid substituted phthalocyanines: Anticancer activity on different cancer cell lines and molecular docking studies

**Ahmet T. Bilgiçli**[1] | **Hayriye Genc Bilgicli**[1] | **Ceylan Hepokur**[2] | **Burak Tüzün**[3] | **Armağan Günsel**[1] | **Mustafa Zengin**[1] | **M. Nilüfer Yarasir**[1]

[1]Department of Chemistry, Sakarya University, Serdivan, Turkey

[2]Department of Basic Pharmaceutical Sciences, Division of Biochemistry, Faculty of Pharmacy, Sivas Cumhuriyet University, Sivas, Turkey

[3]Department of Chemistry, Sivas Cumhuriyet University, Sivas, Turkey

**Correspondence**
Ahmet T. Bilgiçli, Department of Chemistry, Sakarya University, 54140, Esentepe, Serdivan, Turkey.
Email: abilgicli@sakarya.edu.tr

In this study, firstly, (4R)-2-(3-hydroxyphenyl)thiazolidine-4-carboxylic acid (**1**) and (4R)-2-(3-(3,4-dicyanophenoxy)phenyl)thiazolidine-4-carboxylic acid (**2**) were prepared. Then, the novel type metallophthalocyanines (ZnPc (**3**), CuPc (**4**), and CoPc (**5**)) bearing thiazolidine groups in peripheral positions were synthesized using by compound (**2**). The synthesized new compounds (**1–5**) were characterized by the combination of standard spectroscopic methods such as FT-IR, $^{1}$H NMR, $^{13}$C NMR, UV–Vis spectral data, and MALDI-TOF. Aggregation behaviors of peripheral tetra-substituted metallophthalocyanines were investigated in dimethyl sulfoxide (DMSO) media. Fluorescence properties and fluorescence quantum yield of the new type zinc phthalocyanine (**3**) were performed in DMSO at room temperature. The anticancer activity of novel type metallophthalocyanines bearing thiazolidine groups in peripheral positions were investigated on rat glioma cancer (C6), human prostate carcinoma (DU-145), and normal human lung fibroblast (WI-38) cell lines. Finally, the biological and chemical activities of (4R)-2-(3-(3,4-dicyanophenoxy)phenyl)thiazolidine-4-carboxylic acid (**2**) and its novel type metallophthalocyanines (ZnPc (**3**), CuPc (**4**), and CoPc (**5**)) have been compared with many parameters obtained using theoretical methods that are the Gaussian software and molecular docking.

**KEYWORDS**

anticancer activities, DFT, molecular docking, phthalocyanines

## 1 | INTRODUCTION

Cancer is the uncontrolled growth and proliferation of cells. It is the most common cause of death after cardiovascular diseases among all causes of death in developed countries. The World Health Organization (WHO) reports that global cancer deaths, which were 7.9 million in 2007, will increase by 45% to 11.5 million in 2030. In another study by the WHO, it is reported that 10 million new cancer cases will be seen each year and more than 6 million deaths will occur this year.[1] In the treatment of cancer, a wide variety of treatments are applied depending on the tissue in the organism, the physiological state of the tumor, and the character of the tumor. These treatments include chemotherapy, radiotherapy, gene therapy, immunotherapy, and monoclonal antibody therapies. Chemotherapy and radiotherapy are the most common treatment modalities in cancer treatment. In

  

radiotherapy, ionizing radiation is used to damage and kill malignant tumor cells. Radiotherapy is a local approach to tumor therapy and is targeted directly at the tumor mass. Ionizing radiation damages the cells' DNA directly or indirectly with free radical formation and causes the death of the cell.[2] Cancer is the second leading cause of death globally, accounting for one in six deaths when considering all deaths that occurred in 2018. Lung, prostate, colorectal, stomach, and liver cancers are the most common cancers in men, whereas breast, colorectal, lung, cervical, and thyroid cancers are the most common among women. Therefore, it is of great importance to synthesize compounds that have potential to be used in the treatment of cancer and to investigate their potential in this field. One of the promising molecules in this field are phthalocyanine compounds due to capable of mimicking the properties of biologically important molecules such as chlorophyll and hemoglobin.[3]

It is well known that metal porphyrin complexes have a vital role in biological processes. The most important group of the porphyrin class is the phthalocyanines that are known as tetrabenzo[5,10,15,20]tetraazaporphyrins. Phthalocyanines are aromatic N4-macrocyclic compounds that are product of four isoindole units. Phthalocyanines attracted great interest for many application areas because of their high stability and delocalized 18 π-electron system with 16 atoms.[4] The unique properties of phthalocyanines arise from delocalized 18 π-electron cloud, which makes these aromatic macrocyclic compounds applicable in different fields. They are widely used in dyeing due to intense blue-green color.[5] At the same time, they have a wide variety of applications besides their role as colorful dye due to their extraordinary chemical, structural, electronic, and optical properties. Thus, phthalocyanines have been investigated in many high technological applications such as liquid crystal,[6] dye-sensitized photovoltaic solar cells,[7] chemical sensors,[8] organic electronics,[9] and nonlinear optics[10] and is still under investigation. Phthalocyanines are also used in antimicrobial,[11] antioxidant,[12] and photodynamic therapy applications because of their photosensitizer properties.[13] The ability of phthalocyanines to generate singlet oxygen makes them promising for photodynamic therapy.[14] The obtained results show that phthalocyanines have anticancer potential through selective and photoactive performance.[15] Hence, phthalocyanine derivatives containing carboxylic, amino, and hydroxyl groups in peripheral and non-peripheral positions are also being developed as a new generation of photosensitizer compounds.[16]

Nitrogen-containing five-membered heterocyclic compounds are found in the structures of several natural products and pharmaceuticals. Most of them are used as synthetic intermediate products, reactants, ligands, or asymmetric synthesis catalysts. Because their many synthesized derivatives are biologically active, thiazolidine has recently become an increasingly used heterocyclic system.[17] It has often been mentioned in previous studies that thiazolidine derivatives have antibacterial, anticancer, antiviral, and enzyme inhibitor effects. Furthermore, thiazolidine-4-carboxylic acid (TCA) derivatives have been known as structural analogue of proline, which is an essential amino acid for bacteria.[18]

Researchers try to produce many methods and procedures to develop more effective and more powerful drugs. Studies have shown that synthesizing new drugs has become very difficult. Therefore, they began to experiment with the metal complexes of molecules. It should be well known that the biological and chemical activity values of the metal complexes are higher than the ligands.[19,20]

In this study, (4R)-2-(2-hydroxyphenyl)thiazolidine-4-carboxylic acid (**1**) as a thiazolidine derivative synthesized. (4R)-2-(3-(3,4-Dicyanophenoxy)phenyl) thiazolidine-4-carboxylic acid (**2**) as ligand and its peripherally tetra-substituted metallophthalocyanine derivatives (**3–5**) were prepared and characterized by standard spectroscopic methods. The anticancer activity of novel type metallophthalocyanine derivatives (**3–5**) bearing thiazolidine groups in peripheral positions were investigated on C6, DU-145, and WI-38 cell lines. Finally, chemical and biological activity values of compound (**2**) and its novel type metallophthalocyanines (ZnPc (**3**), CuPc (**4**), and CoPc (**5**)) were calculated and compared with Gaussian software program and molecular docking methods.

## 2 | EXPERIMENTAL

### 2.1 | Materials and methods

All the chemical substances used for the synthesis of compounds such as 4-nitrophthalonitrile, 3-hydroxybenzaldehyde, NaOAc, L-cysteine hydrochloride, siligacel, chloroform, acetone, *N*,*N*-dimethylformamide (DMF), tetrahydrofuran (THF), methanol, ethanol, *n*-hexane, toluene, 1,8-diazabicyclo[5.4.0]undec-7-ene (DBU), $K_2CO_3$, $CuCl_2$, Zn $(CH_3COO)_2$, and $CoCl_2$ were provided commercially companies (Merck, Sigma-Aldrich, and Fluka). Fetal bovine serum (FBS), penicillin–streptomycin (PS), and trypsin were purchased from Biological Industries. Dulbecco's Modified Eagle Medium (DMEM) and phosphate buffer saline (PBS) were supplied from Wisent Bio Products. XTT (sodium 3′-[1-[(phenylamino)-carbonyl]-3,4-tetrazolium]-bis(4-methoxy-6-nitro)benzene sulfonic acid hydrate) was purchased from Chemical

Company. FT-IR spectra of synthesized compounds were recorded by PerkinElmer Spectrum Two spectrometer (ATR sampling accessory). This spectrophotometer has UATR Diamond/ZnSe ATR. The FT-IR spectra of novel synthesized compounds were recorded in a 4-$cm^{-1}$ resolution in the range from 600 to 4000 and in four scans. $^{1}H$ and $^{13}C$ NMR spectra were recorded using a Varian 300-MHz Mercury Plus instrument using TMS as internal standards. The ultraviolet–visible (UV–Vis) spectra of new synthesized phthalocyanine derivatives were performed by Agilent Model 8453 diode array UV–Vis spectrometer. Electronic absorbance spectra of new metallophthalocyanines were obtained in wavelength range of 190–1100 nm and slit width of 1-nm optical specifications in dimethyl sulfoxide (DMSO) at room temperature. Fluorescence spectra of compounds were taken by Hitachi S-7000 fluorescence spectrophotometer. Fluorescence emission and excitation spectra of ZnPc were performed in scan speed: 1200, excitation slit: 2.5 nm, and emission slit: 2.5 nm optical specifications in DMSO at room temperature.

## 2.2 | Synthesis

### 2.2.1 | *Synthesis of (4R)-2-(3-hydroxyphenyl)thiazolidine-4-carboxylic acid* (1)

3-Hydroxybenzaldehyde (10 mmol) was dissolved in EtOH (10 mL). To the solution were added L-cysteine hydrochloride (1.57 g, 10 mmol) and NaOAc (0.98 g, 12 mmol) dissolved in water (10 mL). The reaction mixture was then stirred for 24 h at room temperature. The precipitate was then separated by filtration and washed several times with EtOH (Scheme 1). $^{1}H$ NMR (300 MHz, DMSO-$d_6$) δ 7.20–7.05 (m, 2H), 6.97–6.85 (m, 2H), 6.87–6.78 (m, 2H), 6.76–6.68 (m, 1H), 6.69–6.58 (m, 1H), 5.57 (s, 1H), 5.40 (s, 1H), 4.19 (dd, $J$ = 6.8, 4.8 Hz, 1H), 3.86 (ddd, $J$ = 8.4, 7.1, 1.0 Hz, 1H), 3.35 (ddd, $J$ = 10.2, 7.1, 1.0 Hz, 1H),3.26 (ddd, $J$ = 10.2, 7.1, 1.0 Hz, 1H), 3.10 (ddd, $J$ = 10.2, 4.6, 1.0 Hz, 1H), 3.03 (td, $J$ = 10.2, 8.6, 1.0 Hz, 1H); $^{13}C$ NMR (75 MHz, DMSO) δ 173.69, 173.22, 158.14, 157.94, 143.25, 140.76, 130.24, 129.94, 118.53, 118.25, 116.04, 115.27, 114.61, 114.39, 72.39, 71.59, 66.11, 65.62, 39.23, 38.64.

### 2.2.2 | The synthesis of (4R)-2-(3-(3,4-dicyanophenoxy)phenyl) thiazolidine-4-carboxylic acid (2)

2-(3-Hydroxyphenyl)thiazolidine-4-carboxylic acid (**1**) (2.1 g, 5.998 mmol) dissolved in DMF (10 mL) and anhydrous $K_2CO_3$ (1.36 g, 11.95 mmol) were efficiently stirred. After 15 min, 4-nitrophthalonitrile (1.0 g, 5.78 mmol) was added drop by drop to the reaction mixture. The obtained mixture was stirred at 40°C for 48 h. Reaction completion or not was checked by TLC. After the completion of reaction, the reaction mixture was cooled room temperature and poured into ice water. The product precipitated after adding some acid to the medium. The obtained product was filtered and washed with water several times. Further purification was made by chromatography over a silica gel column by using an eluent of $CHCl_3$ (Scheme 1).

2-(3-(3,4-Dicyanophenoxy)phenyl)thiazolidine-4-carboxylic acid (**2**) was soluble in THF, DMSO, and DMF. Yield of (2): 1.46 g (72%). Anal. calcd. for (%) $C_{18}H_{13}N_3O_3S$ (351.38 g $mol^{-1}$): C, 61.53; H, 3.73; N, 11.96; O, 13.66; S, 9.13. Found: C, 61.14; H, 3.79; N, 11.55. FT-IR ($\upsilon_{max}$ $cm^{-1}$): 3200 (carboxylic acid OH), 3094, 3066, 3022 (Ar–CH), 2224 (C≡N), 1655 (C=O), 1581(aromatic C=C), 1474, 1250, 1210, 827, 519. $^{1}H$ NMR (300 MHz, DMSO-$d$) δ 7.95 (d, 1H), 7.82 (d, 1H), 7.56 (d, 1H), 7.46–7.35 (m, 1H), 7.29–7.14 (m, 2H), 6.85–6.78 (8 m, 3H), 6.71 (d, 1H), 6.62 (d, 1H), 5.62 (s, 1H), 5.35 (s, 1H), 4.07 (d, 1H), 3.74 (dd, 1H), 3.23 (dd, 1.0 Hz, 1H),3.14 (dd, 1H), 2.98 (dd, 1H), 2.91 (t, 1H). MS ($m/z$): 352.29 $[M + H]^+$.

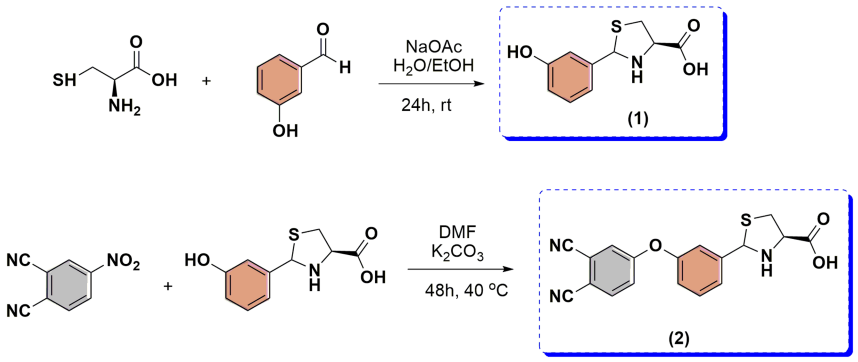


**SCHEME 1** Synthetic route of (4R)-2-(3-(3,4-dicyanophenoxy)phenyl)thiazolidine-4-carboxylic acid (**2**)

### 2.2.3 | General procedure for the synthesis of metallophthalocyanines (3–5)

2-(3-(3,4-Dicyanophenoxy)phenyl)thiazolidine-4-carboxylic acid (**2**) (100 mg, 0.28 mmol) and anhydrous metal salts (Zn (Acac)$_2$, $CuCl_2$, and $CoCl_2$: ~0.030 g, excess) were heated in 140°C temperature for 5 h under $N_2$ atmosphere in hexanol and DBU (0.05 mL) as non-nucleophilic base (Scheme 2). The obtained yellow products were precipitated with hexane and then filtered and washed with MeOH several times. The obtained phthalocyanines were further purified by column chromatography using $CH_2Cl_2$ as eluent. Finally, the obtained new metallophthalocyanines (**3–5**) are soluble in DMF, DMSO, and pyridine.

Yield of (**3**): 29 mg (29%). $C_{72}H_{52}N_{12}O_{12}S_4Zn$ (1470.93 g mol$^{-1}$). Calculated elemental analysis (%); C, 58.79; H, 3.56; N, 11.43; O, 13.05; S, 8.72; Zn, 4.45. Found: C, 58.12; H, 3.72; N, 11.78%. UV–Vis (THF) $\lambda_{max}$: 679 nm (Q-band), 630 nm, 620 nm (n–π*), 351 nm (B-band). FT-IR $\nu$ cm$^{-1}$: 3220, 1654, 1594, 1107, 1095, 739. $^1$H NMR (300 MHz, DMSO-*d*) δ 8.20–7.90 (broad, 12H, Pc–Ar–H), 7.40–6-60 (m, 16H, Ar–H) 5.39 (s, 4H) 5.58 (s, 4H), 4.20 (d, 4H) 3.10 (m, 4H), 2.75(d, 4H), 2.85 (d, 4H). MALDI-MS: *m*/*z*: 1495.03 $[M + Na + H]^+$.

Yield of (**4**): 31 mg (31%). $C_{72}H_{52}N_{12}O_{12}S_4Cu$ (1469.06 g mol$^{-1}$). Calculated elemental analysis (%); C, 58.87; H, 3.57; Cu, 4.33; N, 11.44; O, 13.07; S, 8.73. Found: C, 58.28; H, 3.82; N, 11.75%. UV–Vis (THF) $\lambda_{max}$: 680 nm (Q-band), 619 nm (n–π*), 349 nm (B-band). FT-IR $\nu$ cm$^{-1}$: 3257, 1652, 1582, 1131, 740. MALDI-MS: *m*/*z*: 1594.78 $[M + 2Na + 2\,K + H]^+$.

Yield of (**5**): 27 mg (27%). $C_{72}H_{52}N_{12}O_{12}S_4Co$ (1463.20 g mol$^{-1}$). Calculated elemental analysis (%); C, 59.05; H, 3.58; Co, 4.02; N, 11.48; O, 13.11; S, 8.76%. Found: C, 58.94; H, 3.45; N, 11.63%. UV–Vis (THF) $\lambda_{max}$: 683 nm (Q-band), 617 nm (n–π*), 356 nm (B-band). FT-IR $\nu$ cm$^{-1}$: 3250, 1648, 1570, 1115, 740. MALDI-MS: *m*/*z*: 1543.96 $[M + 2\,K + 2H]^+$.

## 2.3 | Determination of fluorescence quantum yields

The fluorescence quantum yields ($\Phi_F$) of the newly synthesized zinc metallophthalocyanine bearing thiazolidine groups in peripheral positions were determined by comparing the integrated area under the curve of the sample using Equation 1.

$$\Phi_F = \Phi_F(\mathrm{Std})\frac{F \,.\, A_{Std} \,.\, n^2}{F_{Std} \,.\, A \,.\, n^2_{Std}} \quad (1)$$

where $F$ and $F_{std}$ are the areas under the fluorescence curves of the complexes and the standard, respectively; $A$ and $A_{std}$ are the respective absorbance of the sample and the standard at the excitation wavelength; and $n$ and $n_{std}$ are the refractive indices of the solvents used for the sample and standard, respectively. Unsubstituted ZnPc was used as a standard in DMSO where $\Phi_F = 0.20$.[21]

## 2.4 | Biological study

### 2.4.1 | Determination of total antioxidant status (TAS)

A commercial kit manufactured by Rel Assay Diagnostics was used to determine the total antioxidant status (TAS). According to this method, the antioxidants in the sample are reduced from the dark blue-green ABTS radical form to the colorless reduced ABTS form. The change of absorbance at 660 nm is related to the total antioxidant capacity of the sample. The assay was calibrated with the reference substance used as the stable standard antioxidant solution, which is the vitamin E analogue called the Trolox equivalent. TAS measurement was performed according to the kit procedure. After calculating the difference between absorbance, the equation given below is calculated according to Equation 2.[22]

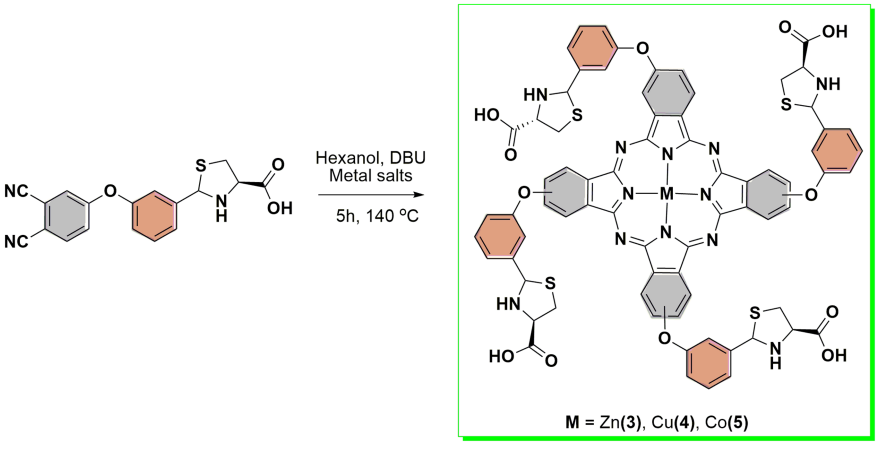


**SCHEME 2** Synthetic route of the novel type metallophthalocyanines (ZnPc (**3**), CuPc (**4**), and CoPc (**5**))

Calculated

$$A_2 - A_1 = \Delta A \qquad x = \frac{\Delta A(\text{sample})}{\Delta A(\text{standart})} x20 \qquad (2)$$

### 2.4.2 | Cell lines

Rat glioma cancer (C6)(ATCC CCL-107), human prostate carcinoma (DU-145) (ATCC HTB-81), and normal human lung fibroblast (WI-38) (ATCC CCL-75) cell lines were from the American Type Culture Collection (ATCC). Cell culture studies of cell lines under appropriate conditions and materials required in order to reproduce broth must be provided. In our study, 10% FBS, 1% L-glutamine, 100 IU $mL^{-1}$ penicillin, and 10 mg $mL^{-1}$ streptomycin in DMEM (high glucose) were used. Cell lines in DMEM was produced in 95% humidity and 5% $CO_2$ incubator at 37°C.

### 2.4.3 | In vitro photodynamic therapy

For photodynamic therapy experiments, healthy and cancer cell lines were incubated in 24-well plates with different concentrations (0–100 μg $mL^{-1}$) of novel type metallophthalocyanine derivatives (ZnPc (**3**), CuPc (**4**), and CoPc (**5**)) for 2–4 h. After incubation, a red diode laser was applied to each well with a light source of 90 mW and a 1-cm radius of light source (670–750 nm) (74 s). All these processes were carried out at room temperature in a dark.

### 2.4.4 | Cytotoxic tests: Determination of $IC_{50}$ dose of compounds in cancer cells

The $IC_{50}$ dose indicates the concentration required to kill 50% of the target of an inhibitor. The $IC_{50}$ dose of the compounds was determined by XTT test using "Cell Proliferation Kit." The XTT kit contains the XTT (2,3-bis (2-methoxy-4-nitro-5-sulfophenyl)-5-[(phenylamino)carbonyl]-2H-tetrazolium hydroxide) agent and the activation agent. XTT solution is prepared by mixing the reagents with 50/1 XTT agent (labeling reagent)/the activation agent (electron coupling reagent). XTT is a tetrazolium salt, but it is converted into water-soluble formazan by dehydrogenase enzyme in mitochondria in cells that are metabolically active. The intensity of the orange color resulting from formazan is proportional to the number of live cells. Cell viability is determined at 475-nm wavelength, depending on the intensity of orange color that occurs after incubation period.[23]

At the end of the process, the $IC_{50}$ value was determined, which was the concentration of the organic compounds that killed half of the cells. Sterilized 96-well plates were seeded with $10^5$ cells per well. Cells were counted using the Olympus R1 cell counting device. Compounds were applied to cells at different concentrations (100.0–50.0–25.0–12.5–6.25–3125 μg $mL^{-1}$). At the end of the incubation period, the compounds were removed from the wells, and XTT kit was applied.

## 2.5 | Theoretical methods

### 2.5.1 | Gaussian study

Bioinformatic chemistry develops and progresses day by day, owing to the developing technology. Chemical and biological activity values of molecules are calculated by bioinformatic chemistry. Owing to these values obtained, it is possible to compare the calculated activity values with the experimental values. Within the scope of this study, GaussView 5.0.8, Gaussian 09 AS64L-G09RevD.01, ChemDraw Professional 15.1, and Chemcraft V1.8 package programs were used in the preparation of molecules.[24–27] Chemical and biological activity values of compound (**2**) and its metallophthalocyanine derivatives (**3–5**) were performed by the Hartree–Fock (HF),[28,29] Becke, three-parameter, Lee–Yang–Parr (B3LYP),[30,31] and M06-2X[32] method with 3-21G, 6-31G, and sdd basis set. As a result of the calculations made on these basis sets, many parameters can be obtained such as $E_{HOMO}$, $E_{LUMO}$, $\Delta E$ (highest occupied molecular orbital [HOMO]–lowest unoccupied molecular orbital [LUMO] energy gap), electronegativity ($\chi$), chemical potential ($\mu$), chemical hardness ($\eta$), electrophilicity ($\omega$), nucleophilicity ($\varepsilon$), global softness ($\sigma$), and proton affinity (PA).[33–36] The ionization energy ($I$) and electron affinity ($A$) of the molecules are related to the HOMO and LUMO values of the molecules. Electronegativity, global softness, and chemical hardness are obtained using the following equations.[37]

$$\mu = -\chi = \left(\frac{\partial E}{\partial N}\right)_{\upsilon(r)} \qquad (3)$$

$$\eta = \frac{1}{2}\left(\frac{\partial^2 E}{\partial N^2}\right)_{\upsilon(r)} = \frac{1}{2}\left(\frac{\partial \mu}{\partial N}\right) \qquad (4)$$

$$\chi = -\mu = \left(\frac{I + A}{2}\right) \qquad (5)$$

$$\eta = \frac{I - A}{2} \qquad (6)$$

It is well known that global softness is defined as the inverse of the chemical hardness.

$$\sigma = 1/\eta \tag{7}$$

$$\chi = -\mu = \left(\frac{-E_{HOMO} - E_{LUMO}}{2}\right) \tag{8}$$

$$\eta = \left(\frac{E_{LUMO} - E_{HOMO}}{2}\right) \tag{9}$$

Electrophilicity and nucleophilicity are important as they are used to the prediction organic and inorganic reaction mechanisms. The global electrophilicity index ($\omega$) that has been investigated by Parr et al.[38] is the inverse of nucleophilicity, and it can be calculated as Equation 10. Nucleophilicity ($\varepsilon$) is defined as the inverse of the electrophilicity like Equation 11.

$$\omega = \mu^2/2\eta = \chi^2/2\eta \tag{10}$$

$$\varepsilon = 1/\omega \tag{11}$$

### 2.5.2 | Docking study

In this study, using the molecular docking method, we tried to calculate the biological activity values of (4R)-2-(3-(3,4-dicyanophenoxy)phenyl)thiazolidine-4-carboxylic acid (**2**) and its novel type metallophthalocyanine derivatives (ZnPc (**3**), CuPc (**4**), and CoPc (**5**)) against different cancer cells such as human galectin-8, protease cancer cells, and brain cancer cells. These cancer cells are composed of many proteins. The compound (**2**) and its metallophthalocyanine derivatives (**3–5**) interacted with these proteins to increase their biological activity.[39] The results of molecular docking calculations were used to compare experimental molecules' biological activities against different cancer cells. *.pdb extension file was obtained using the structure of the optimized molecule with the Gaussian software program.[25] Cancer tissues and molecule files were studied at HEX 8.0.0.[40] About docking displays, help was received from the SeeSAR 9.0 software program.[41]

## 3 | RESULTS AND DISCUSSION

### 3.1 | Spectroscopic characterization of novel type phthalocyanines

The structure of novel type metallophthalocyanines (ZnPc (**3**), CuPc (**4**), and CoPc (**5**)) were characterized by the combination of common spectroscopic technique such as FT-IR, $^1$H NMR, and UV–Vis spectroscopy. All obtained spectra are consistent with the related structures. The synthesized metallophthalocyanines are mixture of four isomers. They cannot easily separate with column chromatography.[42] For this reason, the characterization of novel type metallophthalocyanines (ZnPc (**3**), CuPc (**4**), and CoPc (**5**)) was made in the mixture of four isomers.

Infrared spectroscopy is very simple and useful technique. It is well known that 4-nitrophthalonitrile has characteristic peaks at 1532 and 1350 cm$^{-1}$ due to nitro groups and at 2220 cm$^{-1}$ due to C≡N vibration.43 Peaks belonging to benzene-bound nitro group were not observed after the nucleophilic aromatic substitution reaction between 4-nitrophthalonitrile and (4R)-2-(3-hydroxyphenyl)thiazolidine-4-carboxylic acid. This is a sign of nucleophilic aromatic displacement reaction (Figure 1). The peak belonging to C≡N vibration shifted from 2220 to 2224 cm$^{-1}$ after nucleophilic displacement reaction. Aromatic CH peaks of compound (**2**) were appeared at 3094, 3066, and 3022 cm$^{-1}$. In addition, carbonyl stretch (C=O) was observed at 1655 cm$^{-1}$. The formation of new metallophthalocyanines (ZnPc (**3**), CuPc (**4**), and CoPc (**5**)) from (4R)-2-(3-(3,4-dicyanophenoxy) phenyl)thiazolidine-4-carboxylic acid (**2**) were performed by the disappearance of the −C≡N vibration at 2224 cm$^{-1}$. The other peaks in infrared spectra of new metallophthalocyanines (**3–5**) are similar with the exception of small stretching shifts (Figure 2).

The $^1$H NMR spectra of ligand (**2**) and zinc metallophthalocyanine ZnPc (**3**) were recorded in deuterated DMSO. The $^1$H NMR spectra of CuPc (**4**) and CoPc (**5**) could not be determined due to the presence of paramagnetic copper and cobalt ions.[44] Aromatic protons of compound (**2**) were observed about 8–8.5 ppm, and protons in the thiazolidine ring were appeared about 3 ppm. Although the $^1$H NMR spectrum of ZnPc (**3**) is similar to compound (**2**), protons in aromatic region could be taken as broad peaks due to aggregation of conjugated π-systems at high concentrations.

It is well known that phthalocyanines have characteristic peaks in electronic spectra that are named as Q-band and B-band. Q-bands occur at 650–700 nm (in the visible region) due to π–π* transition, and the blue-green color of the phthalocyanines is related to Q-band transitions. Also, O-bands of phthalocyanines provide information on whether the compounds contain metals in the core or not. Metallophthalocyanine derivatives show only narrow Q-band absorption in electronic spectra due to their $D_{4h}$ symmetry, whereas phthalocyanines with no metal in the center (metal-free phthalocyanine) are observed as two split bands due to change of symmetry from $D_{4h}$ to $D_{2h}$. The other characteristic band, B-bands (Soret

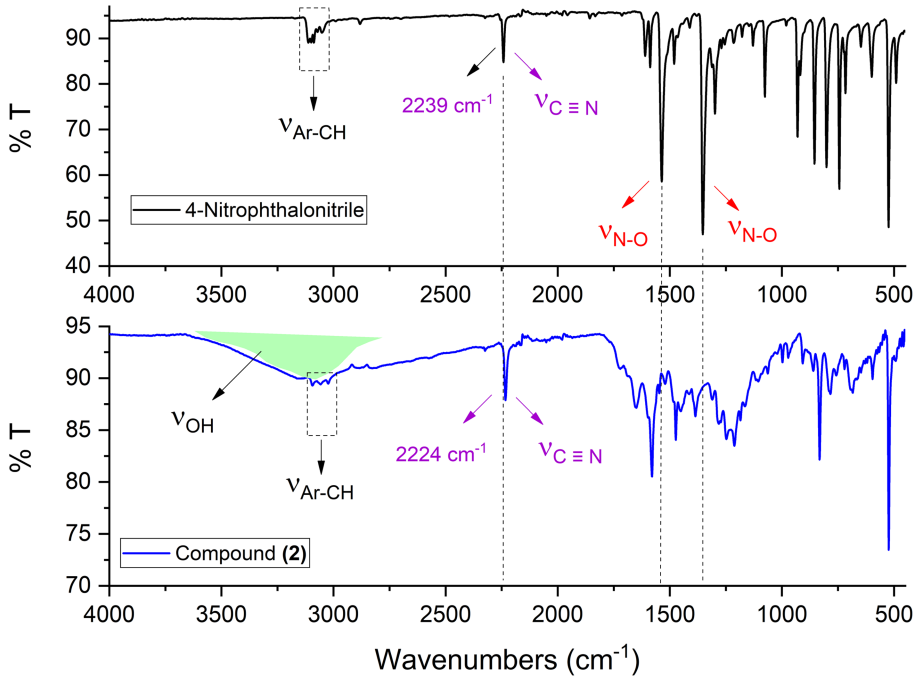


**FIGURE 1** FT-IR spectra of (4R)-2-(3-(3,4-dicyanophenoxy)phenyl) thiazolidine-4-carboxylic acid (**2**) and 4-nitrophthalonitrile

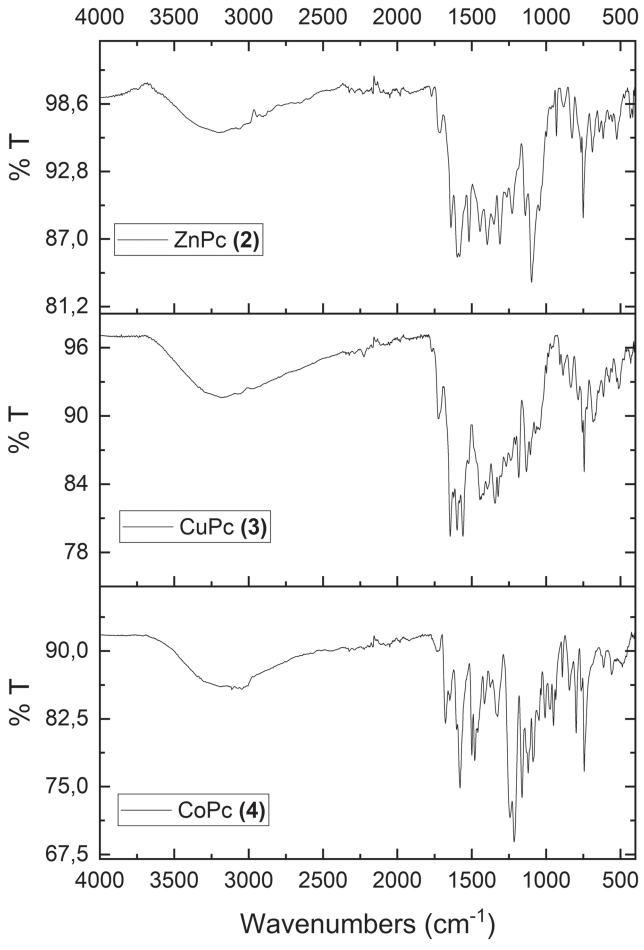


**FIGURE 2** FT-IR spectra of new metallophthalocyanines (ZnPc (**3**), CuPc (**4**), and CoPc (**5**))

bands), is observed at around 300–400 nm (in the UV region) due to deeper π-levels → LUMO transition.

The UV–Vis absorption spectra of synthesized novel type metallophthalocyanines (ZnPc (**3**), CuPc (**4**), and CoPc (**5**)) were observed intense Q-bands at $\lambda_{max}$ 679, 680, and 683 nm as a single band, respectively. The single Q-bands of phthalocyanines are characteristic due to increase of the symmetry with metalation. The Q-bands of phthalocyanines with no metal in the center (metal-free phthalocyanine) were observed as two split bands at $\lambda_{max}$ 667 and 702 nm as expected due to $D_{2h}$ symmetry. The B-bands of these metallophthalocyanines (ZnPc (**3**), CuPc (**4**), and CoPc (**5**)) were appeared at $\lambda_{max}$ 353, 350, and 356 nm, respectively (Figure 3). The B-band of metal-free phthalocyanine is $\lambda_{max}$ 334 nm. The Q- and B-band values in electronic spectra of new metallophthalocyanines are compatible with the literature.

## 3.2 | Aggregation studies

It is well known that phthalocyanines have aggregation tendency due to conjugated 18-π-electron system. The aggregation tendency of phthalocyanine is one of the most problems that hinder use in high technological applications, because the aggregation tendency of phthalocyanines has adverse effect on solubility as well as electrochemical, optical, photophysical, and photochemical properties. However, the aggregation tendency of phthalocyanines can be reduced or prevented by changing

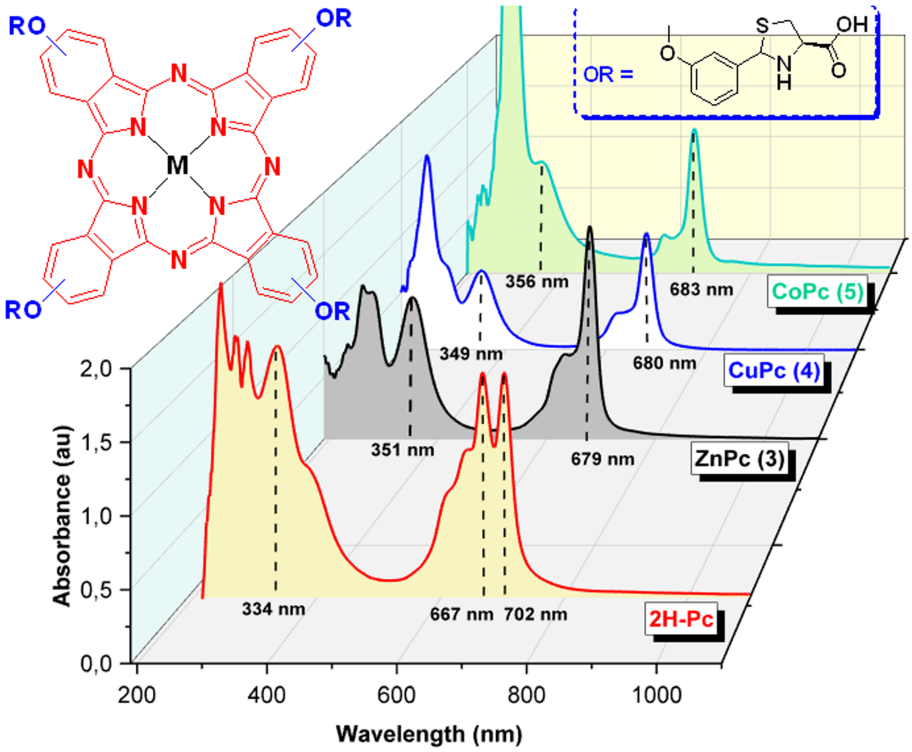


**FIGURE 3** UV–Vis spectra of novel type metallophthalocyanines (ZnPc (**3**), CuPc (**4**), CoPc (**5**), and 2HPc) in DMSO

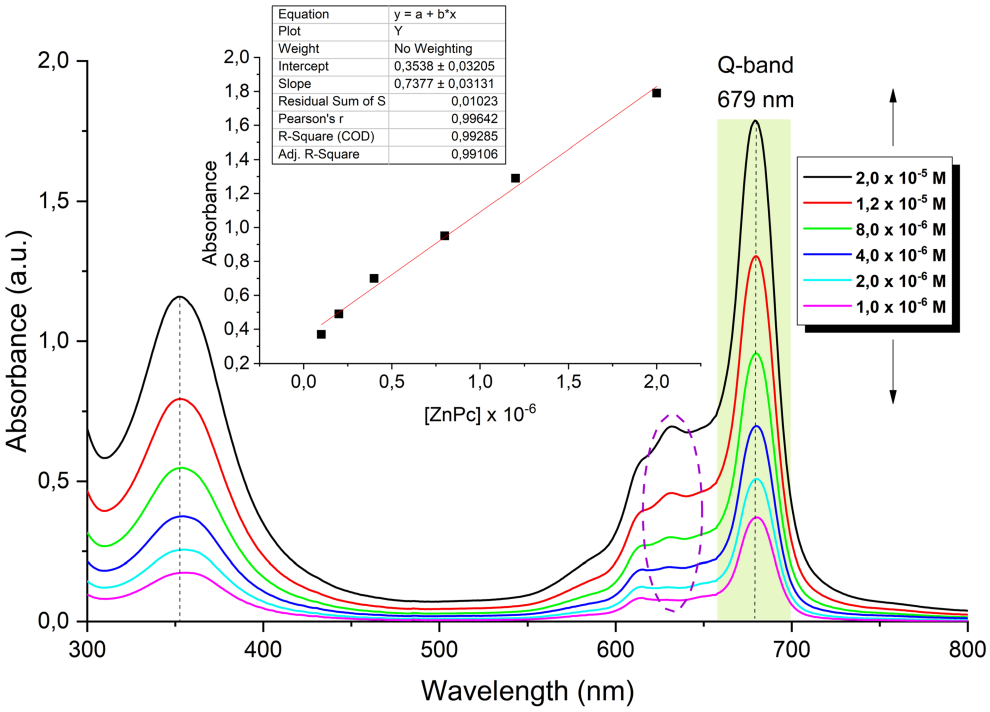


**FIGURE 4** Electronic spectra of ZnPc (**3**) in DMSO at different concentrations

some properties such as solvents, concentration, nature of functional group, and temperature. Two types of aggregation, H-type (face to face) and J-type (edge to edge), are seen in phthalocyanines. H-type aggregation causes the Q-band to shift blue, and J-type aggregation causes it to shift to red. In this study, it tried to determine the effect of binding of (4R)-2-(3-hydroxyphenyl)thiazolidine-4-carboxylic acid groups to the peripheral positions of metallophthalocyanines on aggregation behavior. The aggregation tendency of phthalocyanines has especially effect on characteristic Q-bands about 600–700 nm. The aggregation of phthalocyanines causes the disappearance or widening of the Q-band peak of the monomer. Therefore, the aggregation properties and the HOMO and

LUMO orbital symmetry of phthalocyanines can be easily investigate by UV–Vis spectroscopy. In the light of this information, the aggregation properties of novel type metallophthalocyanines (ZnPc (**3**), CuPc (**4**), and CoPc (**5**)) were performed by UV–Vis spectrophotometry. UV–Vis spectrum of the ZnPc (**3**) at different concentrations was recorded in DMSO (Figure 4). When the concentration of ZnPc (**3**) was increased, the narrow Q-band intensity increased. But when the concentration of ZnPc (**3**) exceeds $2.0 \times 10^{-6}$ M, a small peak occurred at 631 nm due to H-type aggregation tendency. Although the else new band formation and blue-/redshift in Q-band was not observed, ZnPc (**3**) is prone to H-type aggregation in DMSO media. Similarly, the absorption spectra of CuPc (**4**) and CoPc (**5**) were recorded between $1.0 \times 10^{-6}$ and $2.0 \times 10^{-5}$ M concentration in DMSO, and no aggregation bands were observed with increasing concentration (Figure 5 for (**4**) and Figure 6 for (**5**)).

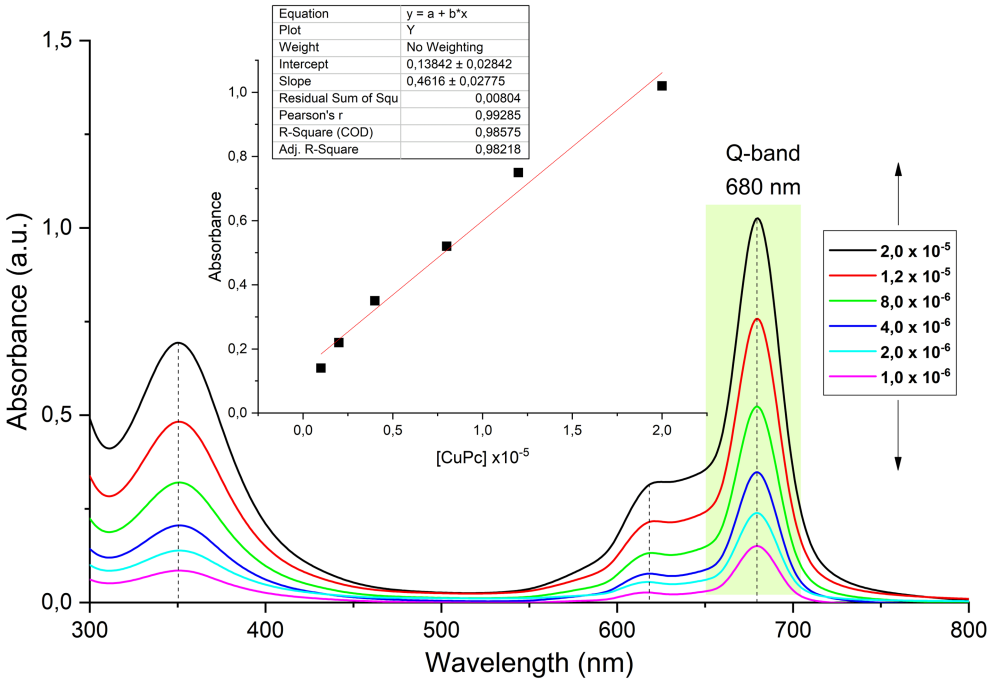


**FIGURE 5** Electronic spectra of CuPc (**4**) in DMSO at different concentrations

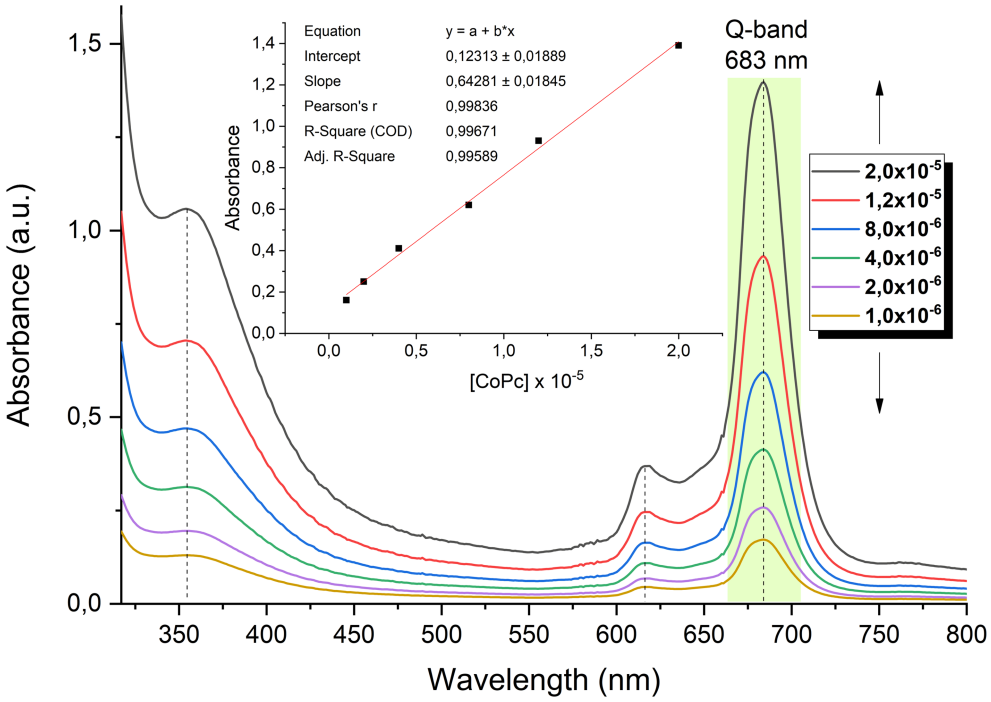


**FIGURE 6** Electronic spectra of CoPc (**5**) in DMSO at different concentrations

### 3.3 | Fluorescence studies

Fluorescence behavior and fluorescence quantum yield of the metallophthalocyanine (ZnPc (**3**)) were investigated by Hitachi S-7000 fluorescence spectrophotometer in DMSO at room temperature. Other new metallophthalocyanines (CuPc (**4**) and CoPc (**5**)) did not show fluorescence behavior because of paramagnetic properties of $Cu^{2+}$ and $Co^{2+}$ ion in the phthalocyanine core. Figure 7 shows the absorption, excitation, and emission spectra of ZnPc (3) in DMSO at room temperature. As seen in Figure 7, the excitation spectrum is similar to absorption spectrum, although the Q-band absorption of ZnPc (**3**) appeared at 675 nm in excitation spectrum ($\lambda_{Exc}$ = 600 nm) and 679 nm in absorption spectrum. Q-band position in excitation spectrum was appeared a little blueshifted (4 nm) compared with absorption spectrum. The fluorescence emission spectrum of ZnPc (**3**) is mirror images of the excitation spectra. This indicates that configuration of the ground and excited states is not affected by excitation in DMSO.[45] The emission peak of ZnPc (**3**) appeared at 688 nm when excited at 650 nm (Table 1). The Stokes shift is 11 nm, which is the usual value for ZnPc derivatives.

It is known that fluorescence emission spectra of some compounds are highly sensitive to pH change due to equilibrium between protonated and non-protonated structure form. Therefore, pH effect on fluorescence

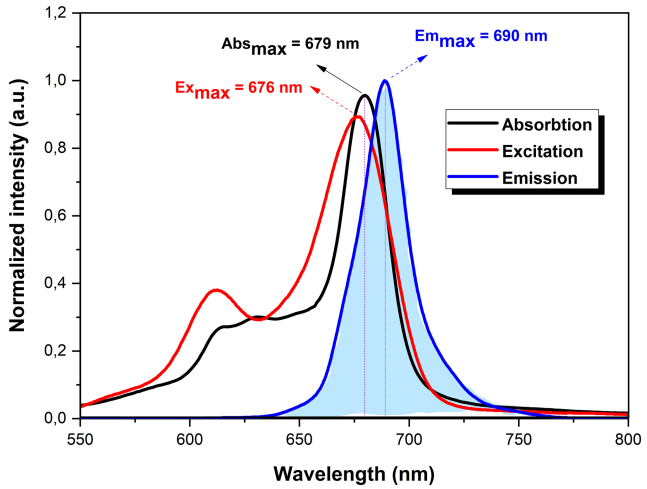


**FIGURE 7** (——) Absorption, (——) excitation, and (——) emission spectra of ZnPc (**3**)

**TABLE 1** Optical and fluorescence properties of the new type metallophthalocyanines (**3–5**) in DMSO

| | UV–Vis | | Fluorescence | | | |
|---|---|---|---|---|---|---|
| **Compound** | $\lambda_{abs}$ (nm) | log $\varepsilon$ cm$^{-1}$ mol$^{-1}$ L | $\lambda_{ex}$ (nm) | $\lambda_{em}$ (nm) | **Stokes shift** | $\Phi_F$ |
| ZnPc (**2**) | 679 | 4.75 | 676 | 690 | 11 | 0.09 |
| CuPc (**3**) | 680 | 4.71 | - | - | - | - |
| CoPc (**4**) | 683 | 4.69 | - | - | - | - |
| ZnPc | 672[a] | 5.38[a] | 672[b] | 682[b] | 10[b] | 0.20[a] |

[a]Ref. [46].
[b]Ref. [21].

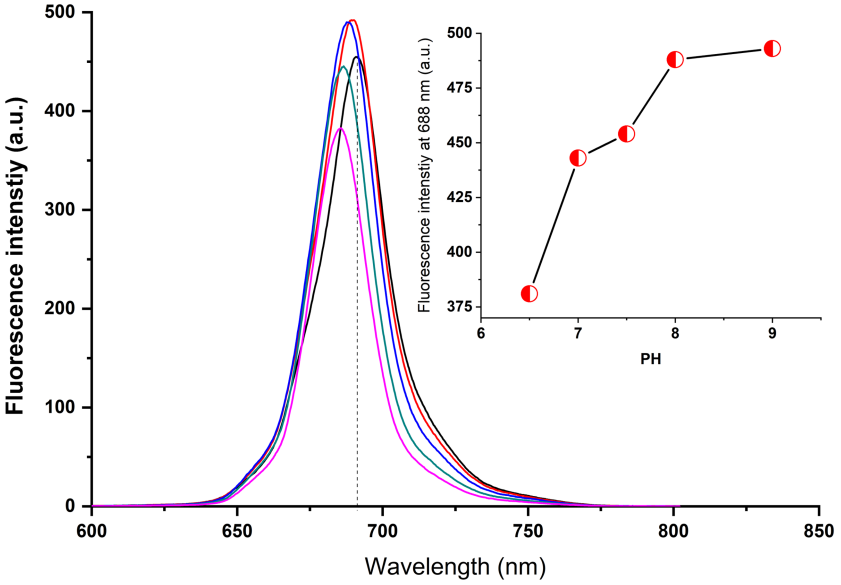


**FIGURE 8** Fluorescence emission spectra of ZnPc (**3**) in different pH values

spectra was investigated in at room temperature. The fluorescence emission spectrum of ZnPc (**3**) was recorded in between 5 and 9 pH values. Emission intensity slightly increased when pH increased from 7 to 9, and at the same time, emission peak at 688 nm was appeared at 686 nm with a little blueshift. On the other hand, when pH increased from 7 to 5, emission intensity slightly decreased, and emission peak at 688 nm appeared at 683 nm with a little blueshift (Figure 8).

It is well known that derivative spectrum gives much detail information about the spectrum. The first derivative spectrum of absorption band gives crossover point as positive maxima and negative minima. When the first derivative of the excitation spectrum of ZnPc (**3**) was taken, the Q-band at 676 nm gave positive maxima bands at 693 nm and negative minima at 663 nm. Shoulder band at 611 and B-band at 351 gave positive maxima bands at 599 and 329 nm and negative minima at 620 and 376 nm, respectively (Figure 9). The second derivative spectrum is characterized by two satellite maxima and an inverted band in which the minimum corresponds to the $\lambda_{max}$ of the fundamental band. When the second derivative of the emission spectrum of ZnPc (**3**) was taken, the emission band at 688 nm gave two satellite maxima at 673 and 698 nm and an inverted band at 685 nm (Figure 10).[46]

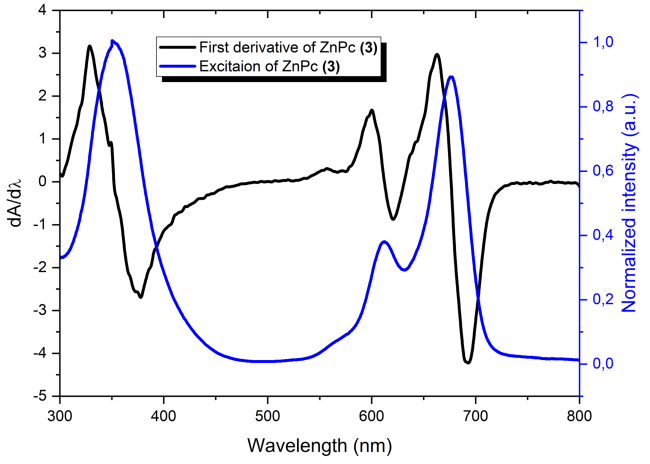


**FIGURE 9** (——) excitation spectrum and (——) first derivative of excitation spectrum of ZnPc (**3**)

The fluorescence quantum yield ($\Phi_F$) of ZnPc (**3**) was calculated according to compared method in the literature. The unsubstituted ZnPc was used as standard compound. The fluorescence quantum yield of unsubstituted ZnPc ($\Phi F_{Std}$) is 0.20.[47] The fluorescence quantum yield ($\Phi_F$) of ZnPc (**2**) was found to be 0.09. The fluorescence quantum yield of ZnPc (**2**) was lower than standard unsubstituted ZnPc. Therefore, it can be said that 2-(3-hydroxyphenyl)thiazolidine-4-carboxylic acid in peripheral positions of ZnPc (**2**) caused a decrease in the fluorescence quantum yield.

## 3.4 | Biological results

In this study, anticancer activity of the novel type metallophthalocyanines (ZnPc (**3**), CuPc (**4**), and CoPc (**5**)) were studied on C6, DU-145, and WI-38 cells. The anticancer activity of the synthesized novel type metallophthalocyanines (ZnPc (**3**), CuPc (**4**), and CoPc (**5**)) was investigated, and obtained results were presented in Table 2. Cells were studied using six concentrations. XTT protocol was applied after 24 h. Viability of control cells has been accepted as %100. It is known that $IC_{50}$ is a

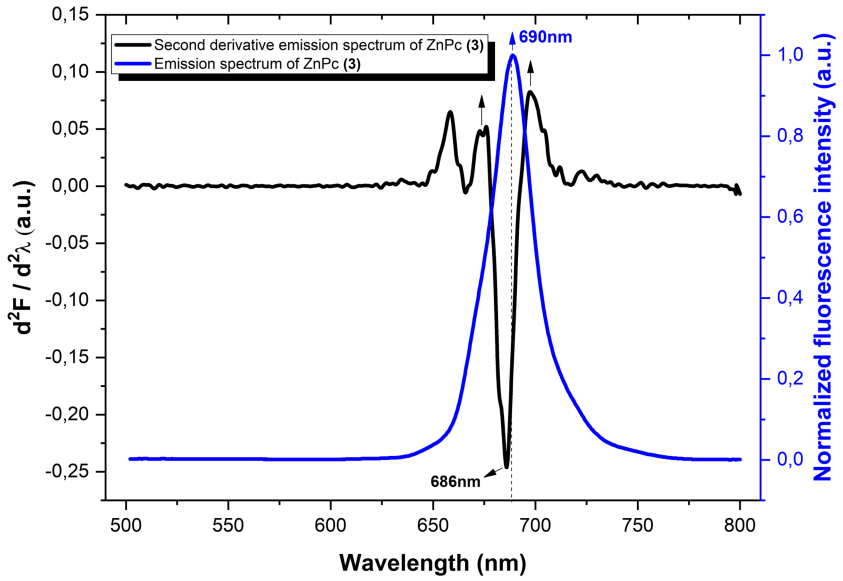


**FIGURE 10** (——) Fluorescence emission and (——) second derivative emission spectra of ZnPc (**3**)

quantitative measure of a drug substance, which inhibits in vitro biological process by 50%, and the concept of $IC_{50}$ is fundamental to pharmacology. Therefore, $IC_{50}$ values of ZnPc (**3**), CuPc (**4**), and CoPc (**5**) were calculated for DU-145, C6, and WI-38 for 24 h. $IC_{50}$ values of ZnPc (**3**) toward human prostate carcinoma (DU-145), rat glioma cancer (C6), and normal human lung fibroblast (WI-38) were found to be 13.82, 7.33, and 3.56 (μg $mL^{-1}$), respectively. When analyzing Table 2, all novel type metallophthalocyanines (**3–5**) have demonstrated anticancer activity on cancer cells. Although observed for ZnPc (**3**) in DU-145, C6, and WI-38 cell lines, CuPc (**4**) has the best activity for rat glioma cancer (C6) lines. According to the obtained experimental results, all synthesized novel type metallophthalocyanines (ZnPc (**3**), CuPc (**4**), and CoPc (**5**)) might be potential candidates for the application in the field of cancer treatment.

**TABLE 2** $IC_{50}$ values of novel type metallophthalocyanine compounds in cell lines

| $IC_{50}$ (μg $mL^{-1}$) | ZnPc (3) | CuPc (4) | CoPc (5) |
|---|---|---|---|
| DU-145 | 3.56 ± 0.024 | 9.70 ± 0.047 | 5.33 ± 0.016 |
| **C6** | 7.33 ± 1.65 | 13.94 ± 0.98 | 3.25 ± 0.025 |
| WI-38 | 13.82 ± 1.36 | 19.94 ± 0.96 | 18.79 ± 0.68 |

**TABLE 3** Total antioxidant (TAS) values

| | ZnPc (3) | CuPc (4) | CoPc (5) |
|---|---|---|---|
| (mmol Trolox equiv. $L^{-1}$) | 6.59 | 1.36 | 3.22 |

The total antioxidant capacity values greater than or equal to 2.0 are considered as high. Total antioxidant capacity values of novel type metallophthalocyanines (ZnPc (**3**), CuPc (**4**), and CoPc (**5**)) are 6.59, 1.36, and 3.22, respectively. Antioxidant capacity of ZnPc (**3**) was found to be highest among synthesized novel type metallophthalocyanine compounds with 6.59 value (Table 3).

## 3.5 | Calculation results

The biological and chemical activities of compound (**2**) and its metal complexes (**3–5**) were compared with Gaussian and molecular docking methods. Previous experimental and theoretical studies have shown that the biological and chemical activities of metal complexes are higher than their ligands.[48–50] Many quantum chemical parameters can be obtained from the Gaussian package program to compare the chemical activity values of molecules. The activity of the molecules can be compared using these obtained parameters. HOMO and LUMO are the most important of these quantum chemical parameters. HOMO and LUMO values give information about the activity of molecule or complex.[51–54] The calculated quantum chemical parameters of compound (**2**) and its metal complexes (**3–5**) in different basis sets such as $E_{HOMO}$, $E_{LUMO}$, $\Delta E$ (HOMO–LUMO energy gap), electronegativity ($\chi$), chemical potential ($\mu$), chemical hardness ($\eta$), electrophilicity ($\omega$), nucleophilicity ($\varepsilon$), global softness ($\sigma$) and PA, the ionization energy ($I$), and electron affinity ($A$) were summarized in Table 4. In the evaluation of calculated

**TABLE 4** Quantum chemical parameters calculated for different basis sets

| | $E_{HOMO}$ | $E_{LUMO}$ | $I$ | $A$ | $\Delta E$ | $\eta$ | $\sigma$ | $\chi$ | Pİ | $\omega$ | $\varepsilon$ | Dipole | Energy |
|---|---|---|---|---|---|---|---|---|---|---|---|---|---|
| B3LYP/6-31G level | | | | | | | | | | | | | |
| (**2**) | −7060 | −2317 | 7060 | 317 | 4742 | 2371 | 0.422 | 4688 | −4688 | 4635 | 0.216 | 6813 | −40,307,072 |
| ZnPc (**3**) | −5045 | −2858 | 5045 | 2858 | 2187 | 1093 | 0.915 | 3952 | −3952 | 7141 | 0.140 | 7319 | −163,019,649 |
| CuPc (**4**) | −5023 | −2834 | 5023 | 2834 | 2189 | 1094 | 0.914 | 3928 | −3928 | 7051 | 0.142 | 2498 | −166,572,236 |
| CoPc (**5**) | −5043 | −2811 | 5043 | 2811 | 2232 | 1116 | 0.896 | 3927 | −3927 | 6911 | 0.145 | 7318 | −165,183,427 |
| HF/6-31G level | | | | | | | | | | | | | |
| (**2**) | −9851 | 1338 | 9851 | −1338 | 11,189 | 5594 | 0.179 | 4256 | −4256 | 1619 | 0.618 | 10954 | −40,107,064 |
| ZnPc (**3**) | −5561 | −0137 | 5561 | 0.137 | 5424 | 212 | 0.369 | 2849 | −2849 | 1496 | 0.668 | 9162 | −162,160,134 |
| CuPc (**4**) | −7310 | 1044 | 7310 | −1044 | 8354 | 4177 | 0.239 | 3133 | −3133 | 1175 | 0.851 | 5833 | −165,741,688 |
| CoPc (**5**) | −7274 | 1054 | 7274 | −1054 | 8329 | 4164 | 0.240 | 3110 | −3110 | 1161 | 0.861 | 4462 | −164,356,879 |
| M062X/6-31G level | | | | | | | | | | | | | |
| (**2**) | −8457 | −1458 | 8457 | 1458 | 6999 | 3500 | 0.286 | 4958 | −4958 | 3512 | 0.285 | 9152 | −40,294,983 |
| ZnPc (**3**) | −5839 | −2337 | 5839 | 2337 | 3501 | 1751 | 0.571 | 4088 | −4088 | 4773 | 0.209 | 3471 | −162,967,764 |
| CuPc (**4**) | −5839 | −2342 | 5839 | 2342 | 3497 | 1748 | 0.572 | 4091 | −4091 | 4786 | 0.209 | 3499 | −166,525,160 |
| CoPc (**5**) | −5858 | −2320 | 5858 | 2320 | 3538 | 1769 | 0.565 | 4089 | −4089 | 4725 | 0.212 | 3319 | −165,134,888 |

results, according to the energy value of the HOMO parameter, the chemical activity values of the compound (**2**) and its metal complexes (**3–5**) are ordered as CuPc (**4**) > CoPc (**5**) > ZnPc (**3**) > compound (**2**). On the other hand, if the chemical activity values of the molecules are sorted according to the LUMO energy value, it is ZnPc (**3**) > CuPc (**4**) > CoPc (**5**) > compound (**2**).

As a result of the calculations, HOMO and LUMO representations of compound (**2**) and its metal complexes (**3–5**) are given in Figure 11. All pictures in Figure 11 have been obtained from the calculations made on the HF/6-31G basis set. It will be seen from these figures that although the HOMO and LUMO orbitals are on the central atoms in ZnPc (**3**) and CoPc (**5**), they are on the edge atoms in the CuPc (**4**) and compound (**2**). The ESP figures show the electrostatic charge distributions of molecules. In these figures, the red regions are electron rich, whereas the blue regions are electron poor.

The numerical values of the quantum chemical parameters obtained as a result of the Gaussian calculations show that the calculations made on the HF/6-31G basis set are the most compatible with both docking results and experimental results.

All the parameters obtained from the calculations are calculated from the HOMO and LUMO energy values. The rankings of others parameter will be obtained in

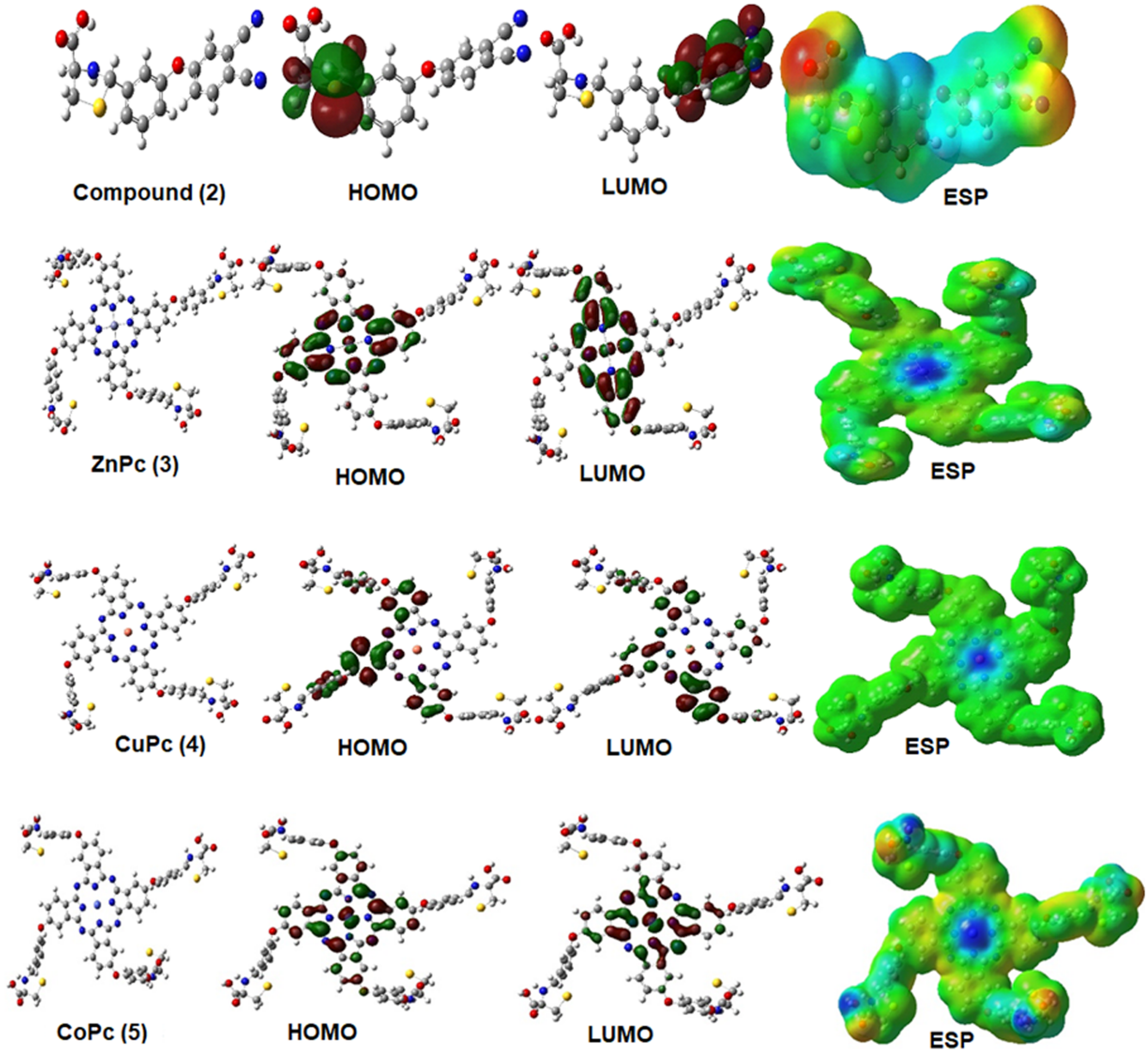


**FIGURE 11** HOMO, LUMO, and ESP representations of (4R)-2-(3-(3,4-dicyanophenoxy)phenyl)thiazolidine-4-carboxylic acid (**2**) and its novel type metallophthalocyanines (ZnPc (**3**), CuPc (**4**), and CoPc (**5**))

similar to the others. Another method is molecular docking, in which the biological activity values of molecules against proteins are calculated. In order to compare the biological activity values of compound (**2**) and its metal complexes (**3–5**), it is necessary to sort by the total energy parameter obtained from docking calculations. For compound (**2**) and its metal complexes, the molecule with the lowest total energy value has the highest biological activity value. In this study, the names of the cancer cells studied were, respectively, *C*-terminal domain of human galectin-8, whose ID was 3OJB; protease-like domain from two-chain hepatocyte growth factor, whose ID was 1SI5; and human glioma pathogenesis-related protein 1 in brain cancer, wherein the ID is 3Q2R. The interaction of cancer cells with compound (**2**) and its metal complexes (**3–5**) is illustrated in Figures 12–14.

Molecular docking total energy values of compound (**2**) and its metal complexes (**3–5**) were calculated for human galectin-8, protease cancer cells, and brain cancer cells. The obtained results were given in Table 5. When the total energy parameter was examined, the biological activity values of compound (**2**) toward human galectin-8, protease

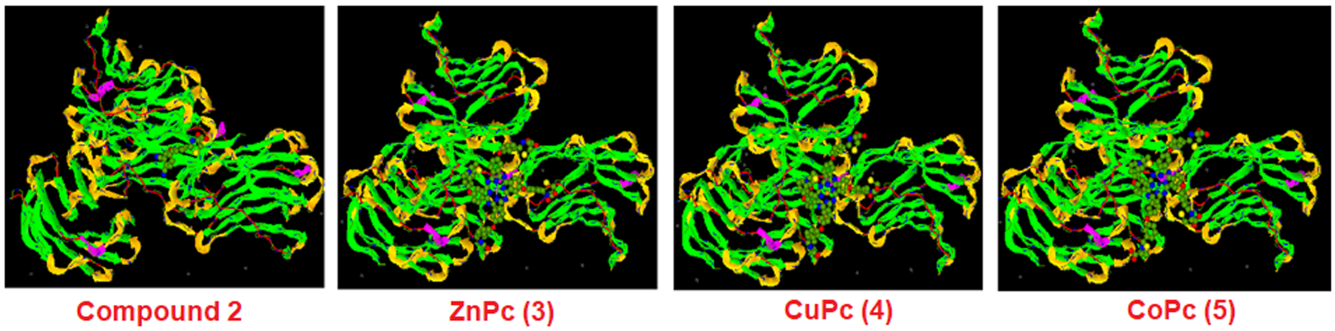


**FIGURE 12** Representation of the interaction of (4R)-2-(3-(3,4-dicyanophenoxy)phenyl)thiazolidine-4-carboxylic acid (**2**) and its novel type metallophthalocyanines (ZnPc (**3**), CuPc (**4**), and CoPc (**5**)) with human galectin-8

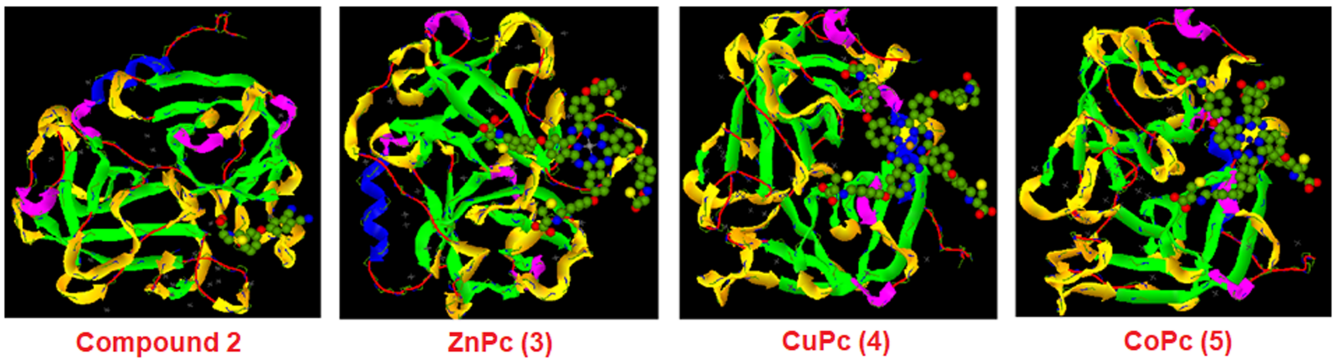


**FIGURE 13** Representation of the interaction of (4R)-2-(3-(3,4-dicyanophenoxy)phenyl)thiazolidine-4-carboxylic acid (**2**) and its novel type metallophthalocyanines (ZnPc (**3**), CuPc (**4**), and CoPc (**5**)) with protease cancer cells

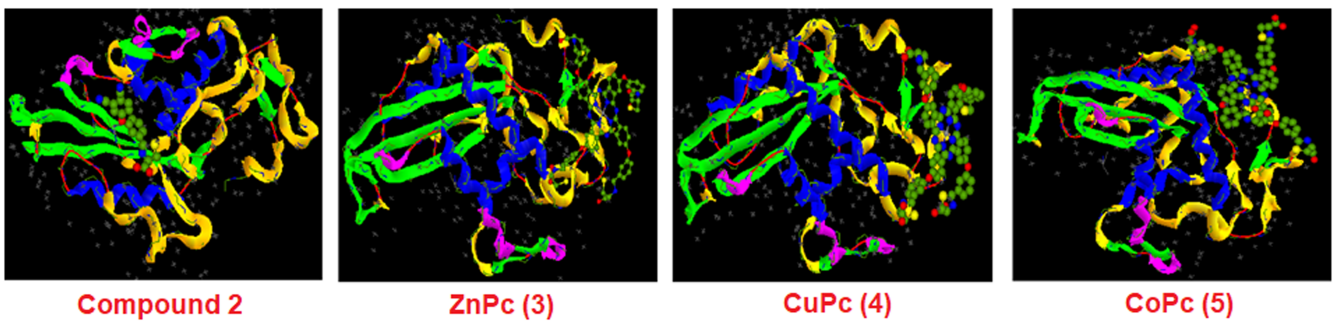


**FIGURE 14** Representation of the interaction of (4R)-2-(3-(3,4-dicyanophenoxy)phenyl)thiazolidine-4-carboxylic acid (**2**) and its novel type metallophthalocyanines (ZnPc (**3**), CuPc (**4**), and CoPc (**5**)) with brain cancer cells

cancer cells, and brain cancer cells were calculated to be −286.05, −270.87, and −282.74 kJ $mol^{-1}$, respectively. These values for new metallophthalocyanines between −503.89 and −558.76 kJ $mol^{-1}$. That is, molecular docking total energy values of metallophthalocyanines (**3–5**) are about twice as high as compared with compound (**2**). When the total energy values of ZnPc (**3**), CuPc (**4**), and CoPc (**5**) are examined, ZnPc (**3**) showed the lowest energy value against the three proteins. Accordingly, whereas ZnPc (**3**) has the highest biological activity, compound (**2**) has the lowest biological activity among them.

As a result of molecular docking calculations, when the total energy parameter was examined, biological activity values of compound (**2**) and phthalocyanine derivatives (**3–5**) were compared. According to the obtained results, ZnPc (**3**) has highest biological activity among them. On the other hand, lowest biological activity was calculated for compound (**2**). Total energy values of compound (**2**) and its phthalocyanine derivatives (**3–5**) against the three proteins summarized in Table 5.

Biological activity of new compounds (2–5) for human galectin-8, protease cancer cells, and brain cancer cells were found as ZnPc (3) > CoPc (5) > CuPc (4) > compound (2). These values showed that the biological activity value of metal complexes (**3–5**) is higher than their ligand molecule (compound (**2**)). The major reason for this is that the contact of compound (**3–5**) is very large; as the contact surface of the molecules increases, the biological activity value may increase.[55,56] Increased contact surface of molecules increases the interaction between molecules and proteins. These interactions are hydrogen bonds, polar and hydrophobic interactions, and π–π and halogen bonds. It should be well known that the effects of these interactions on the biological activity values of molecules are great.[57–59]

When the biological activity values of the compound (**2**) and the quaternary form of compound (**2**) against human galectin-8 proteins are compared, it is seen that the quaternary form of compound (**2**) has a higher biological activity value than the compound (**2**) in Figures 15

**TABLE 5** Molecular docking total energy values for compound (**2**) and its phthalocyanine derivatives (**3–5**)

| | Human galectin-8 | Protease cancer cells | Brain cancer cells |
|---|---|---|---|
| Compound (**2**) | −286.05 | −282.74 | −270.87 |
| ZnPc (**3**) | −558.76 | −545.10 | −520.25 |
| CuPc (**4**) | −504.45 | −522.21 | −503.89 |
| CoPc (**5**) | −510.64 | −530.82 | −511.37 |

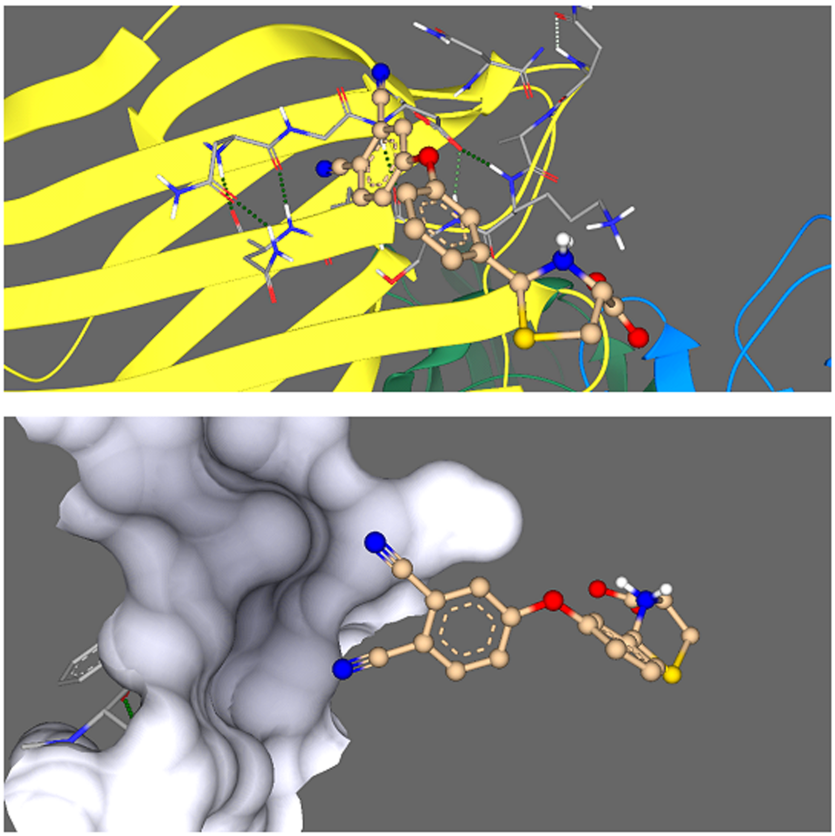

**FIGURE 15** Representation of the interaction of (4R)-2-(3-(3,4-dicyanophenoxy) phenyl)thiazolidine-4-carboxylic acid (**2**) with human galectin-8

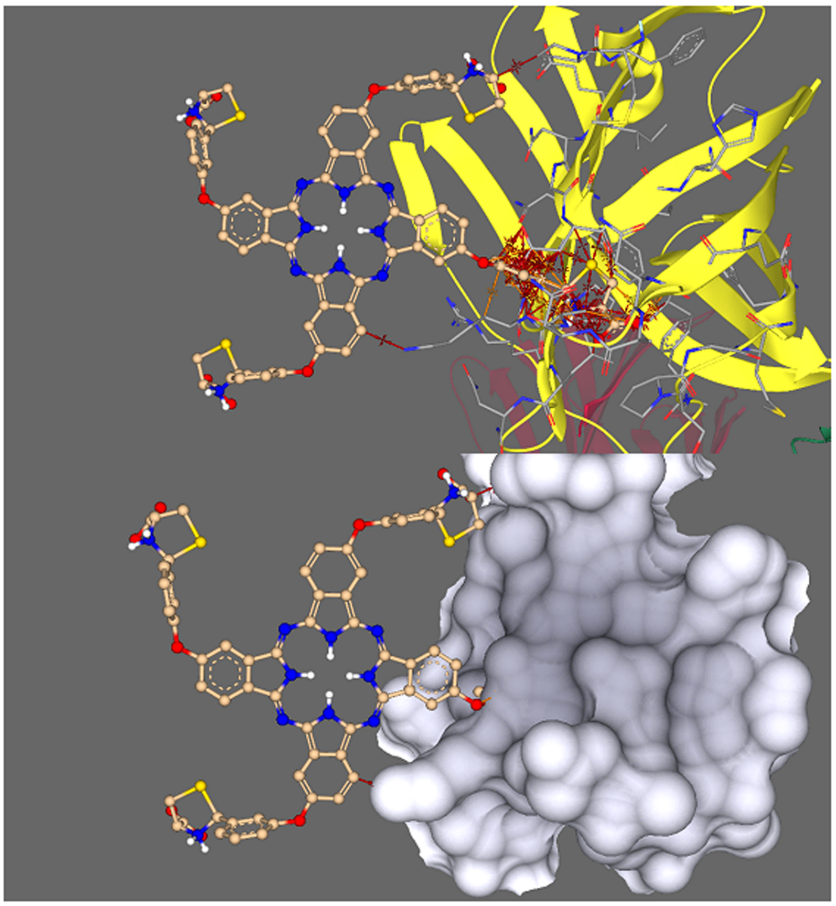

**FIGURE 16** Representation of the interaction of the quaternary form of (4R)-2-(3-(3,4-dicyanophenoxy)phenyl)thiazolidine-4-carboxylic acid (**2**) with human galectin-8

**TABLE 6** Docking parameters of compound (**2**) and its quaternary form against human galectin-8

| | Compound (2) | Quaternary form of compound (2 ) |
|---|---|---|
| hERG $pIC_{50}$ | 3.559 | 2.577 |
| logP | −0.520 | 2.978 |
| logS | 2.410 | 0.170 |

and 16. SeeSAR 9.0 software program was used to compare these two molecules in Table 6.[60–62] When the parameters obtained as a result of this comparison are examined, it shows that the hERG $pIC_{50}$ value of the quaternary form of compound (**2**) is lower and the biological activity value of the quaternary form of compound (**2**) is higher. Other parameters are logP and logS. LogS gives information about the solubility of molecules. The logS value of molecules gives information about how it dissolves in water. In clinical studies, this feature provides important information about the distribution of drugs used in the body and drug delivery methods. The logP value is the coefficient of separation. This parameter gives information about the ability of molecules to cross a biological membrane.

## 4 | CONCLUSION

In this study, 2-(3-(3,4-dicyanophenoxy)phenyl) thiazolidine-4-carboxylic acid and its peripheral tetra-substituted novel type metallophthalocyanines (ZnPc (**3**), CuPc (**4**), and CoPc (**5**)) were successfully prepared. The synthesized compounds were characterized by standard spectroscopic methods. The aggregation behaviors of novel type metallophthalocyanines were investigated by UV–Vis spectrophotometer. According to electronic spectra recorded between $1.0 \times 10^{-6}$ and $2.0 \times 10^{-5}$ M concentration in DMSO, the synthesized metallophthalocyanine compounds did not show aggregation behaviors. The fluorescence quantum yield of ZnPc (**3**) was found to be 0.09. It is seen that the fluorescence quantum yield decreased compared with unsubstituted phthalocyanine complexes.

The anticancer activity of the novel type metallophthalocyanines derivatives (**3–5**) was studied by using six concentrations (3.125; 6.25; 12.5; 50; 75; 100 μg $mL^{-1}$) on C6, DU-145, and WI-38 cell lines. The best activity was observed for ZnPc (**3**) with 3.56 μg $mL^{-1}$ in DU-145 cells. In anticancer studies, ZnPc (**3**) was found to possess potent activity against the two tested cancer cell lines. In the study, $IC_{50}$ values in DU-145 cell line were found to

be 3.56, 9.70, and 5.33 for ZnPc (**3**), CuPc (**4**), and CoPc (**5**), respectively. $IC_{50}$ values in C6 cell line were found to be 7.33, 13.94, and 5.33 for ZnPc (**3**), CuPc (**4**), and CoPc (**5**), respectively. $IC_{50}$ values in DU-145 cell line were found to be 3.56, 9.70, and 5.33 for ZnPc (**3**), CuPc (**4**), and CoPc (**5**), respectively. Although the $IC_{50}$ values of ZnPc (**3**), CuPc (**4**), and CoPc (**5**) are effective in cancer cell lines at low doses, approximately three times higher in the healthy cell line indicates that the anticancer activity of the compounds is good. According to the results obtained, preliminary structure–activity relationship showed that peripheral tetra-substituted ZnPc (**3**) was the most active member in this study, which revealed antitumor activity against DU-145 and C6 cell lines. According to the obtained results from this study, ZnPc (**3**) must be further studied in the DNA level to know their mode of action. In light of these results, focus on the synthesis of various new ZnPc derivatives will be worked in the future. In addition, the ZnPc application in PDT will be investigated at various different cell lines in various concentrations.

Total antioxidant capacity values of novel type metallophthalocyanines (ZnPc (**3**), CuPc (**4**), and CoPc (**5**)) are 6.59, 1.36, and 3.22, respectively. The biological and chemical activities of 2-(3-(3,4-dicyanophenoxy)phenyl) thiazolidine-4-carboxylic acid (**2**) and its novel type (**3–5**) have been compared with many parameters obtained using theoretical methods such as Gaussian software and molecular docking. Theoretical studies showed that novel type metallophthalocyanines (**3–5**) have higher biological activity than 2-(3-(3,4-dicyanophenoxy)phenyl) thiazolidine-4-carboxylic acid (**2**). In both DFT and molecular docking studies, ZnPc (**3**) has the highest chemical and biological activity value. According to obtained results from experimental and theoretical studies, the synthesized novel type metallophthalocyanines **(3–5)** might be potentially candidates for the application in the field of cancer treatment.

## ACKNOWLEDGMENTS

This research was made possible by TUBITAK ULAKBIM High Performance and Grid Computing Center (TR-Grid e-Infrastructure).

## AUTHOR CONTRIBUTIONS

**Ahmet T. Bilgiçli:** Conceptualization; data curation; investigation; methodology; resources, writing-original draft; writing-review & editing. **Hayriye Genç Bilgiçli:** Conceptualization; data curation; investigation; methodology; writing-original draft. **Ceylan Hepokur:** Conceptualization; data curation; formal analysis; investigation; methodology. **Burak Tüzün:** Data curation; formal analysis; investigation; methodology; resources; software. **Armağan Günsel:** Data curation; formal analysis; investigation; methodology. **Mustafa Zengin:** Data curation; formal analysis; investigation; methodology. **M. Nilüfer Yaraşır:** Data curation; investigation; methodology.

## DATA AVAILABILITY STATEMENT

The data that support the findings of this study are available from the corresponding author upon reasonable request.

## ORCID

*Ahmet T. Bilgiçli* https://orcid.org/0000-0002-4144-7357
*Hayriye Genc Bilgicli* https://orcid.org/0000-0001-6909-316X
*Ceylan Hepokur* https://orcid.org/0000-0001-6397-1291
*Burak Tüzün* https://orcid.org/0000-0002-0420-2043
*Armağan Günsel* https://orcid.org/0000-0003-1965-1017
*Mustafa Zengin* https://orcid.org/0000-0002-0243-1432
*M. Nilüfer Yarasir* https://orcid.org/0000-0002-7327-7137

## REFERENCES

[1] R. Chouhan, A. K. Baipai, *Journal of Nanobiotechnology* **2009**, *7*, 1.
[2] S. C. Sak, P. Harnden, C. F. Johnston, A. B. Paul, A. E. Kiltie, *Clinical Cancer Research* **2005**, *11*(17), 6205.
[3] E. H. Alici, A. T. Bilgiçli, A. Günsel, G. Arabaci, M. N. Yarasir, *Dalton Trans.* **2021**, *50*, 3224.
[4] C. C. Leznoff, A. B. P. Lever (Eds), *Phthalocyanines: Properties and Applications*, Vol. 3, John Wiley & Sons Inc., Cambridge, UK **1993**.
[5] M. Urbani, M. E. Ragoussi, M. Khaja Nazeeruddin, T. Torres, *Coord. Chem. Rev.* **2019**, *381*, 1.
[6] T. Basovai, A. Hassan, M. Durmus, A. G. Gürek, V. Ahsen, *Coord. Chem. Rev.* **2016**, *310*, 131.
[7] T. Keleş, Z. Biyiklioglu, E. Güzel, M. Nebioğlu, I. Şişman, *Appl. Organomet. Chem.* **2021**, *35*, e6076.
[8] L. Valli, *Adv. Colloid Interface Sci.* **2005**, *116*, 13.
[9] A. Günsel, A. T. Bilgiçli, B. Tüzün, H. Pişkin, M. N. Yarasir, B. Gündüz, *New J. Chem.* **2020**, *44*, 369.
[10] G. de la Torres, P. Vazquez, F. Agullo-Lopez, T. Torres, *J. Mater. Chem.* **1998**, *8*, 1671.
[11] A. Günsel, A. Kobyaoğlu, A. T. Bilgiçli, B. Tüzün, B. Tosun, G. Arabaci, M. N. Yarasir, *J. Mol. Struct.* **2020**, *1200*, 127127.
[12] A. T. Bilgicli, Y. Tekin, E. H. Alici, M. N. Yaraşir, G. Arabaci, M. Kandaz, *J. Coord. Chem.* **2015**, *68*(22), 4102.
[13] X. Li, B. D. Zheng, X. H. Peng, S. Z. Li, J. W. Ying, Y. Zhao, J. D. Huang, J. Yoon, *Coord. Chem. Rev.* **2019**, *379*, 147.
[14] B. Habermeyer, R. Guilard, *Photochem. Photobiol. Sci.* **2018**, *17*, 1675.
[15] N. Shirasu, S. O. Nam, M. Kuroki, *Anticancer Res.* **2013**, *33*(7), 2823.
[16] S. Kudrevich, N. Brasseur, C. La Madeleine, S. Gilbert, J. E. van Lier, *J. Med. Chem.* **1997**, *40*(24), 3897.

[17] M. J. Naim, M. J. Alam, S. Ahmad, F. Nawaz, N. Shrivastava, M. Sahu, O. Alam, *Eur. J. Med. Chem.* **2017**, *129*, 218.
[18] V. Gududuru, E. Hurh, J. T. Dalton, D. D. Miller, *J. Med. Chem.* **2005**, *48*, 2584.
[19] S. Kaya, B. Tüzün, C. Kaya, I. B. Obot, *J. Taiwan Inst. Chem. Eng.* **2016**, *58*, 528.
[20] B. Tüzün, C. Kaya, *Journal of Bio-and Tribo-Corrosion* **2018**, *4* (4), 69.
[21] E. T. Saka, M. Durmus, H. Kantekin, *J. Organomet. Chem.* **2011**, *696*, 913.
[22] O. Erel, *Clin. Biochem.* **2004**, *37*(4), 277.
[23] E. Üstün, A. Özgür, K. A. Coskun, S. D. Düşünceli, İ. Özdemir, Y. Tutar, *Transition Met. Chem.* **2017**, *42*, 331.
[24] R. Dennington, T. Keith, J. Millam, GaussView, version 6, Semichem Inc., Shawnee Mission, KS, USA **2016**.
[25] M. J. Frisch, G. W. Trucks, H. Schlegel, G. E. Scuseria, M. A. Robb, J. R. Cheeseman, G. Scalmani, V. Barone, B. Mennucci, G. A. Petersson, H. Nakatsuji, M. Caricato, X. Li, H. P. Hratchian, A. F. Izmaylov, J. Bloino, G. Zheng, J. L. Sonnenberg, M. Hada, M. Ehara, K. Toyota, R. Fukuda, J. Hasegawa, M. Ishida, T. Nakajima, Y. Honda, O. Kitao, H. Nakai, T. Vreven, J. A. Montgomery Jr., J. E. Peralta, F. Ogliaro, M. Bearpark, J. J. Heyd, E. Brothers, K. N. Kudin, V. N. Staroverov, R. Kobayashi, J. Normand, K. Raghavachari, A. Rendell, J. C. Burant, S. S. Iyengar, J. Tomasi, M. Cossi, N. Rega, J. M. Millam, M. Klene, J. E. Knox, J. B. Cross, V. Bakken, C. Adamo, J. Jaramillo, R. Gomperts, R. E. Stratmann, O. Yazyev, A. J. Austin, R. Cammi, C. Pomelli, J. W. Ochterski, R. L. Martin, K. Morokuma, V. G. Zakrzewski, G. A. Voth, P. Salvador, J. J. Dannenberg, S. Dapprich, A. D. Daniels, O. Farkas, J. B. Foresman, J. V. Ortiz, J. Cioslowski, D. J. Fox, Gaussian 09, revision D.01, Gaussian, Inc., Wallingford, CT, USA **2009**.
[26] PerkinElmer, ChemBioDraw Ultra version (13.0.0.3015), CambridgeSoft, Waltham, MA, USA **2012**.
[27] Chemissan version 4.43 package, **2016**
[28] D. Vautherin, D. M. Brink, *Physical Review C* **1972**, *5*(3), 626.
[29] A. D. Becke, *The Journal of Chemical Physics* **1993**, *98*(7), 5648.
[30] P. J. Stephens, F. J. Devlin, C. F. N. Chabalowski, M. J. Frisch, *J. Phys. Chem.* **1994**, *98*(45), 11623.
[31] K. B. Wiberg, *J. Comput. Chem.* **2004**, *25*(11), 1342.
[32] E. G. Hohenstein, S. T. Chill, C. D. Sherrill, *J. Chem. Theory Comput.* **2008**, *4*(12), 1996.
[33] S. Kaya, P. Banerjee, S. K. Saha, B. Tüzün, C. Kaya, *RSC Adv.* **2016**, *6*(78), 74550.
[34] B. Tüzün, *Turkish Computational and Theoretical Chemistry* **2018**, *2*(1), 12.
[35] B. Tüzün, *Cumhuriyet Science Journal* **2019**, *40*(2), 396.
[36] B. Tüzün, *Journal of New Results in Science* **2014**, *3*(5), 67.
[37] L. E. Brus, *The Journal of Chemical Physics* **1983**, *79*(11), 5566.
[38] R. G. Parr, W. Yang, *Density Functional Theory of Atoms and Molecules*, Oxford University Press, Oxford, UK **1989**.
[39] Z. Bikadi, E. Hazai, *Aust. J. Chem.* **2009**, *1*, 15.
[40] D. Ritchie, Hex 8.0. 0 user manual, **1996**.
[41] LeadIT version 2.3.2; BioSolveIT GmbH, Sankt Augustin, Germany, **2017**, www.biosolveit.de/LeadIT
[42] N. B. McKeown, *Phthalocyanine Materials: Synthesis, Structure and Function*, Cambridge University Press, Cambridge, UK **1998**.
[43] A. Yahyazadeh, V. Azimi, *Elixir Appl. Chem.* **2012**, *49*, 9991.
[44] Ü. Demirbaş, D. Akyüz, B. Barut, R. Bayrak, A. Koca, H. Kantekin, *Spectrochim. Acta, Part a* **2016**, *153*, 71.
[45] E. Kırbaç, A. Erdoğmuş, *J. Mol. Struct.* **2020**, *1202*, 127392.
[46] R. Bayrak, H. T. Akçay, F. Ş. Beriş, E. Şahin, H. Bayrak, Ü. Demirbaş, *Spectrochim. Acta, Part a* **2014**, *133*(10), 272.
[47] A. Ogunsipe, J.-Y. Chen, T. Nyokong, *New J. Chem.* **2004**, *28* (7), 822.
[48] I. Ali, W. A. Wani, K. Saleem, M. F. Hseih, *Polyhedron* **2013**, *56*, 134.
[49] K. Saleem, W. A. Wani, A. Haque, M. N. Lone, M. F. Hsieh, M. A. Jairajpuri, I. Ali, *Future Med. Chem.* **2013**, *5*(2), 135.
[50] I. Ali, W. A. Wani, K. Saleem, M. F. Hsieh, *RSC Adv.* **2014**, *4* (56), 29629.
[51] J. I. Aihara, *The Journal of Physical Chemistry a* **1999**, *103*(37), 7487.
[52] C. Caicedo, G. Zaragoza-Galán, J. Crusats, Z. El-Hachemi, A. Martínez, E. Rivera, *J. Porphyrins Phthalocyanines* **2014**, *18* (03), 209.
[53] N. A. Sánchez-Bojorge, S. Flores-Armendáriz, M. E. Fuentes-Montero, V. H. Ramos-Sánchez, G. Zaragoza-Galán, L. M. Rodríguez-Valdez, *J. Porphyrins Phthalocyanines* **2017**, *21* (02), 88.
[54] N. A. Sánchez-Bojorge, G. Zaragoza-Galán, N. R. Flores-Holguín, M. A. Chávez-Rojo, C. Castro-García, L. M. Rodríguez-Valdez, *J. Mol. Struct.* **2019**, *1191*, 259.
[55] A. Kosiha, K. M. Lo, C. Parthiban, K. P. Elango, *Mater. Sci. Eng., C* **2019**, *94*, 778.
[56] L. Ozalp, S. S. Erdem, B. Yüce-Dursun, Ö. Mutlu, M. Özbil, *Comput. Biol. Chem.* **2018**, *77*, 87.
[57] A. Atasever, H. Ozdemir, I. Gulcin, O. I. Kufrevioglu, *Food Chem.* **2013**, *136*(2), 864.
[58] M. Şentürk, İ. Gülçin, M. Ciftci, Ö. İ. Küfrevioğlu, *Biol. Pharm. Bull.* **2008**, *31*(11), 2036.
[59] İ. Gülçin, Ö. İ. Küfrevioğlu, M. Oktay, *J. Enzyme Inhib. Med. Chem.* **2005**, *20*(3), 297.
[60] M. Imber, V. V. Loi, S. Reznikov, V. N. Fritsch, A. J. Pietrzyk-Brzezinska, J. Prehn, J. Hamilton, C. Wahl, M. C. Bronowska, K. Agnieszka, H. Antelmann, *Redox Biology* **2018**, *15*, 557.
[61] I. Sagud, I. Skoric, D. Vuk, A. Ratkovic, F. Burcul, *Turk. J. Chem.* **2019**, *43*(4), 1170.
[62] P. Morgan, M. Mangal, C. W. Lin, *International Research Journal of Pharmacy and Medical Sciences* **2018**, *2*(1), 13.

**How to cite this article:** Bilgiçli AT, Genc Bilgicli H, Hepokur C, et al. Synthesis of (4R)-2-(3-hydroxyphenyl)thiazolidine-4-carboxylic acid substituted phthalocyanines: Anticancer activity on different cancer cell lines and molecular docking studies. *Appl Organomet Chem*. 2021;35:e6242. https://doi.org/10.1002/aoc.6242